NUMERICAL SIMULATION ON EMITTANCE GROWTH CAUSED BY ROUGHNESS OF A METALLIC PHOTOCATHODE

Z. Zhang, C. Tang*, Tsinghua University, Beijing 100084, China

Abstract

The roughness of a photocathode could lead to an additional uncorrelated divergence of the emitted electrons and therefore to an increased thermal emittance. The randomness of the real-life photocathode surface makes it unrealistic to perform typical beam dynamics simulation to study the roughness emittance growth. We develop a numerical simulation code based on the point spread function (PSF) and an estimated form of electric field distribution on an arbitrary gently undulating surface to deal with the problem. The simulation result shows that the emittance growth factor is 1.04, which is much smaller than expected ($1.5 \sim 2$).

INTRODUCTION

Photocathodes are widely integrated in large particle sources. The quantum efficiency (QE) and intrinsic emittance determine the quality of the photocathode. D. Dowell gives formulas [1] to predict the QE and thermal emittance of a metallic smooth surface photocathode by using a simplified three-step model [2]:

$$QE(\omega) \approx \frac{1 - R(\omega)}{1 + \frac{\lambda_{opt}}{\lambda_{e-e}(\omega)}} \frac{(\hbar\omega - \phi_{eff})^2}{8\phi_{eff}(E_F + \phi_{eff})}$$

$$\varepsilon_{n,x} = \sigma_x \sqrt{\frac{\hbar\omega - \phi_{eff}}{3mc^2}}$$

Formula for QE agrees well with the experiments, while the emittance measured by some labs appeared to be two times larger than predicted [3,4]. It's widely believed that the differ between the experiment and analysis is caused by surface roughness of the photocathode.

Typical beam dynamics simulations require the electric field distribution in the simulation region as well as the initial particle samples. However it's hard to acquire on an arbitrary photocathode surface due to the computer memory and CPU limitation.

In this paper, we developed a numerical simulation code based on the point spread function (PSF) and an estimated form of electric field distribution on an arbitrary gently undulating surface to deal with the issues.

PRINCIPLES OF THE SIMULATION

Generation of the Initial Particle Samples

The keypoint of initial samples generation is how one include the emission angle diffusion introduced by the surface roughness, which is also known as "slope effect" [5,6]. This can be done in at least two ways:

_____

* tang.xuh@tsinghua.edu.cn

1. Employ the similar three-step model as discussed in [1] and use the Monte Carlo method. Considering the emission process as shown in Fig. 1. One photon injected into a gentle slope on the bulk metal photocathode, travelling a distance of s along $-z$ direction, then absorbed by an electron of energy E, went towards surface with a direction angle (θ', ϕ') relative to the normal of the slope (the slope angle is θ) without scattering and finally escaped from the surface.
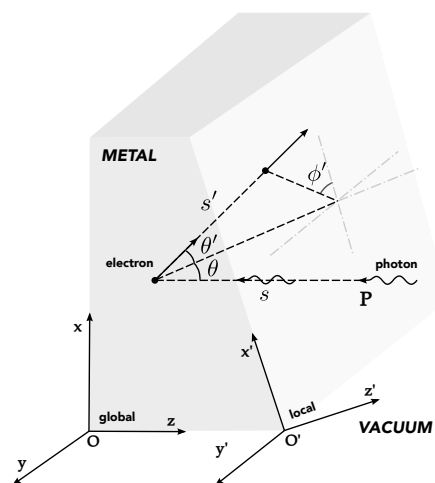
Figure 1: The schematic plot for the bulk photoemission on a part of a rough metallic cathode. The definitions of coordinates and variables are labeled in the plot.

The idea is to generate $s \sim \text{Exp}(\lambda)$, $E \sim U(E_F - \hbar\omega, E_F)$, $\theta' \sim U(0, \pi/2)$, $\phi' \sim U(0, 2\pi)$, where $1/\lambda = 1/\lambda_{opt} + 1/\bar{\lambda}_{e-e}$, then apply the filter condition $(E + \hbar\omega)\cos^2\theta' \geq \phi_{eff}$ to eliminate samples that cannot escape. All definitions of the parameters above are in consistence with [1]. However the sampling efficiency of this simple method is very low due to the fact that the QE of metal is usually $\sim 10^{-4}$.

2. Employ the point spread function (PSF) of the photocathode. In general, the PSF describes the response of an imaging system to a point source or point object. For photocathode, the PSF describes the response of a photocathode to a point laser source. With the PSF of photocathode, one could generate the samples without large loss (to be specified, our sampling pass rate is around $1/6$, which will be explained later), therefore we choose the second sampling method.

The generalized momentum PSF For typical photoemission on metallic cathode, it's safe to ignore the dependence between electron momentum distribution and incident

position. The phase space distribution of emitted electrons D can be simplified as $D \approx I(x_0, y_0) f_p(p_x, p_y, p_z)$ where $I(x_0, y_0)$ is the intensity of the photon incident position and f_p the momentum PSF. With this assumption, we derived the generalized momentum PSF for oblique incidence case as shown below (p_x, p_y, p_z in local frame in Fig. 1):

$$f_p(p_x, p_y, p_z) = \frac{C_p(\theta) p_z}{\sqrt{p_z^2 + p_m^2} \cdot \sqrt{p_x^2 + p_y^2 + p_z^2 + p_m^2}}$$

$$C_p(\theta) = \frac{1 - R(\theta)}{1 + \dfrac{\lambda_{\text{opt}}}{\lambda_{e-e}} \cos\theta} \cdot \frac{1}{4\pi m \hbar \omega}$$

for clarity we omitted the Heaviside functions. For typical metals, $C_p(\theta)$ varies slow with θ when $\theta < 1\,\text{deg}$, thus we take $C_p(\theta)$ as a constant in the simulation. Since f_p is only valid in local frame, we generate the samples in the local frame, then apply the rotation matrix to transform the samples to the global frame.

Sampling from the generalized momentum PSF The full 6-D phase space distribution of the initial beam could be separated into two parts: the spatial part $S(x, y, z)$ and the momentum part $f_p(p_x, p_y, p_z)$. We apply the rejective method [7] to perform effective sampling for the momentum part.

It's known that the number of samples generated for every accepted sample obeys geometric distribution $G(p)$. Therefore the expected value of N is $1/p$. For our case, $E(N)$ satisfies:

$$E(N) = \pi \left(1 + \frac{p_m}{p_M}\right)$$

where $p_m = \sqrt{2m(E_F + \phi_{\text{eff}})}$ and $p_M = \sqrt{2m(E_F + \hbar\omega)}$. Since p_m is very close to p_M in typical bulk photoemission, we get $E(N) \approx 2\pi \approx 6$.

The Electric Field Distribution on an Arbitrary Gently Undulating Surface

To simulate the "field effect" [5, 6, 8, 9] which occurs when applying the rf field on the surface of photocathode, one need to generate the electric field distribution on the arbitrary surface. However it's unrealistic to do this in field simulation program (such as superfish and CST) since it's too memory consuming. Fortunately, for "gently undulating surface"[1], there exist some approximate formulas for the electric field distribution, which is proved to be accurate enough for our case.

Assume that the 3-D surface morphology function is $z = R(x, y)$, we choose the base plane so that $\langle R(x, y) \rangle = 0$. Suppose that the electric field potential between the cathode surface $z = R(x, y)$ and infinity $z = +\infty$ has the approximate form:

$$\phi(x, y, z) = z + \int dk_x dk_y C(k_x, k_y) \cdot e^{j(k_x x + k_y y) - kz}$$

---

[1] A "gently undulating surface" means that *most* of the slopes of the spatial frequency components of the surface should be much smaller than 1.

where $k = \sqrt{k_x^2 + k_y^2}$. The form above automatically satisfies the Laplace's equation and B.C. at infinity. By applying the B.C. at the cathode surface, in regard of first order approximation, one could get that $C(k_x, k_y) = -R(k_x, k_y)$ where $R(k_x, k_y)$ is the coefficient of Fourier transformation of $R(x, y)$. So the electric potential could be written as:

$$\phi(x, y, z) = z - \int dk_x dk_y R(k_x, k_y) \cdot e^{j(k_x x + k_y y) - kz}$$

Thus the electric field has the form:

$$E_x = j \int dk_x dk_y \cdot k_x R(k_x, k_y) \cdot e^{j(k_x x + k_y y) - kz}$$

$$E_y = j \int dk_x dk_y \cdot k_y R(k_x, k_y) \cdot e^{j(k_x x + k_y y) - kz}$$

$$E_z = -1 - \int dk_x dk_y \cdot k R(k_x, k_y) \cdot e^{j(k_x x + k_y y) - kz}$$

The accuracy of the above formulas could be verified by comparing the surface morphology and the calculated potential map as shown in Fig. 2.

The Motion Equations of the Emitted Beam

We employ the 5th order Runge-Kutta method to do the motion equation integration. For technical reasons, we prefer using the distance from baseplane z as the integration variable rather than time t. The electron motion equation about z could be written as:

$$\frac{dp_x\,[\text{keV/c}]}{dz\,[\text{nm}]} = 511 \times 10^{-6} \cdot \frac{E_0\,[\text{MV/m}]}{p_z\,[\text{keV/c}]} \cdot \hat{E}_x(x, y, z)$$

$$\frac{dx\,[\mu\text{m}]}{dz\,[\text{nm}]} = \frac{p_x\,[\text{keV/c}]}{p_z\,[\text{keV/c}]} \cdot 1 \times 10^{-3}$$

where x stands for both x and y direction, E_0 is the electric field strength, and $\hat{E}_x$ is the transverse normalized electric field distribution. Note that for convenience, we use μm as the length unit for transverse direction but nm for longitudinal direction.

Knowing that the transverse components of the electric field will vanish as the distance to the surface baseplane goes up, the transverse momentum of the emitted electron would be saturated at a large z (typically around 5000 nm). We will do statistics at that position to get the emittance growth factor to compare with the experimental results.

SIMULATION RESULTS

Our simulation configuration is shown in Fig. 3, the details could be found in the caption. The parameters used in the simulation is shown in Table 1.

The simulation result is shown in Fig. 4. In Fig. 4 one could see that, the phase space is distorted along x direction. The distortion is caused by the transverse electric field on the surface, and this distortion introduces the emittance growth.

Doing statistics on both the initial phase space and the final one, we obtain that the emittance growth factor is $\eta_s = \varepsilon_f / \varepsilon_i = \frac{4.826\,\mu\text{m} \cdot \text{keV/c}}{4.623\,\mu\text{m} \cdot \text{keV/c}} = 1.044$. Surprisingly the emittance growth factor is far smaller than expected ($1.5 \sim 2$)!
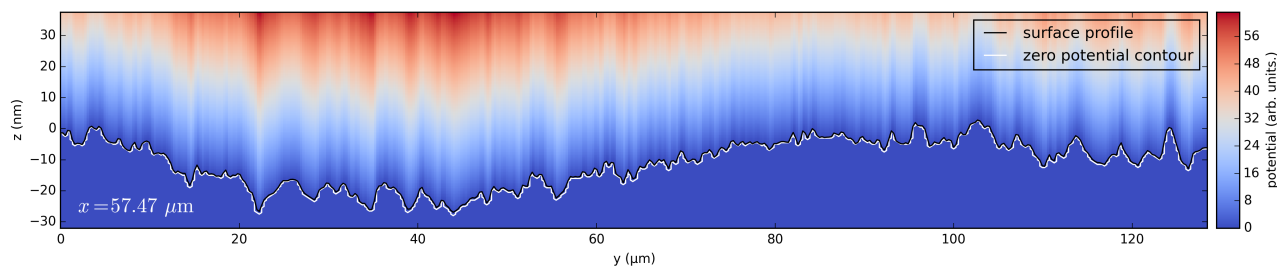
Figure 2: Validation of the accuracy of the analytical electric potential. The surface profile along $x = 57.47\,\mu m$ (in Fig. 3) is marked by the black bold curve. The white bold curve in the plot is the zero potential contour of the analytical electric potential in the y-z plane at $x = 57.47\,\mu m$, which is calculated by the equations. In the plot, the surface profile and the zero potential contour are mostly overlapped, therefore we conclude that the analytical electric potential is quite accurate.
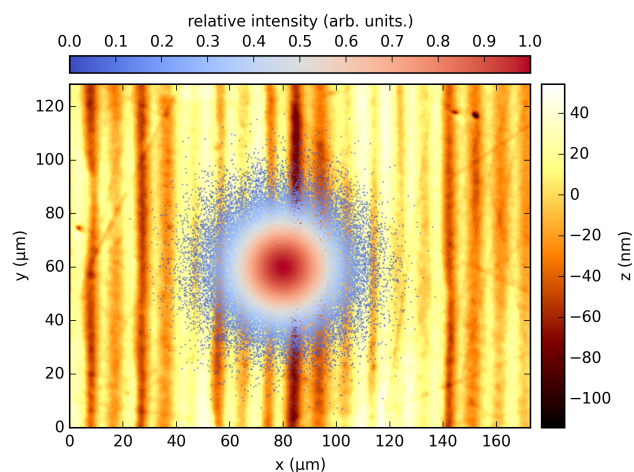
Figure 3: Simulation configuration. The yellow-black background shows the morphology of the surface, and the blue-red spot describes the intensity distribution of the laser.

Figure 4: Simulated evolution of the horizontal phase space and emittance of the electron beam generated from the rough copper surface (Fig. 3). Upper left: the initial phase space at $z = 0\,nm$; Upper right: the final phase space at $z = 5000\,nm$; Bottom: the evolution of ε_x along z.

Table 1: Parameters Used in Numerical Simulation

Parameter	Value	Description
λ_l	266.0 nm	laser wavelength
l-dist	uniform	laser transverse distribution
r_l	20.0 μm	laser transverse radius
x_l	80.0 μm	laser incident x center
y_l	60.0 μm	laser incident y center
mat	copper	material of the cathode
E_0	50.0 MV/m	electric field strength
ϕ_w	4.31 eV	work function
ϕ_{eff}	4.04 eV	effective work function
E_F	7.0 eV	Fermi energy
N	10000	number of particles
z_i	0 nm	simulation starting position
z_f	5000.0 nm	simulation ending position
dz	10.0 nm	simulation z step

CONCLUSION

In this paper, we described the details of a numerical simulation code that we developed to simulate the emittance evolution of an electron beam generated on a real-life rough surface photocathode. From the simulation results, we surprisingly found that for 3-D random surface of a real-life photocathode, the influence of the surface roughness to the emittance growth is much smaller than expected.

ACKNOWLEDGMENT

REFERENCES

[1] D. H. Dowell and J. F. Schmerge. Quantum efficiency and thermal emittance of metal photocathodes. *Physical Review Special Topics-Accelerators and Beams*, 12(7):074201, 2009.

[2] D. Dowell, F. King, R. Kirby, J. Schmerge, and J. Smedley. In situ cleaning of metal cathodes using a hydrogen ion beam. *Physical Review Special Topics-Accelerators and Beams*, 9(6):063502, 2006.

[3] H. Qian. *Research on the Emittance Issues of Photocathode RF Gun*. PhD thesis, Tsinghua University, April 2012.

[4] H. Qian. Experimental investigation of thermal emittance components of copper photocathode. *Physical Review Special Topics - Accelerators and Beams*, 15(4), 2012.

[5] X. He, C. Tang, W. Huang, and Y. Lin. Researches on thermal emittance of metal cathode in photoinjectors. *High Energy Phys. Nucl. Phys.*, 28(9):1007–1012, Sep 2004.

[6] K. Flottmann. Note on the thermal emittance of electrons emitted by cesium telluride photo cathodes. 1997.

[7] D. Ghosh and A. Vogt Drawing a sample from a given distribution. In *Proceedings of JSM 2008 Conference, Denver, Colorado*, pages 1048–1051, 2008.

[8] Y. Y. Lau. Effects of cathode surface roughness on the quality of electron beams. *Journal of applied physics*, 61(1):36–44, 1987.

[9] M. Krasilnikov. Impact of the cathode roughness on the emittance of an electron beam. In *Proceedings of FEL 2006 Conference, Berlin, Germany*, pages 583–586, 2006.